Mass spectrometry (fragmentation ratios) of DNA base molecules following 80 keV proton impact with separation of direct ionization and electron capture processes

J. Tabet, S. Eden, S. Feil, H. Abdoul-Carime, B. Farizon, M. Farizon, S. Ouaskit, T.D. Märk

Mass spectrometry (fragmentation ratios) of DNA base molecules following 80 keV proton impact with separation of direct ionization and electron capture processes

J. Tabet[a], S. Eden[a,1], S. Feil[a], H. Abdoul-Carime[a], B. Farizon[a], M. Farizon[a], S. Ouaskit[b], T. D. Märk[c]

[a]Université de Lyon, F-69003, Lyon, France; Université Lyon 1, Villeurbanne; CNRS/IN2P3, UMR5822, Institut de Physique Nucléaire de Lyon; F-69622 Villeurbanne

[b]Université Hassan II-Mohammédia, Faculté des Sciences Ben M'Sik (LPMC), B.P.7955 Ben M'Sik, Casablanca, Morocco

[c]Institut für Ionenphysik und Angewandte Physik, Leopold Franzens Universität, Technikerstrasse 25, A-6020 Innsbruck, Austria

Abstract

The first fragmentation ratios are presented for the ionization and dissociative ionization of gas-phase DNA bases following 80 keV (1.8 v_0) proton impact. Event-by-event determination of the projectile charge state after collision enables also to distinguish the relative contributions of electron capture (EC) by the projectile from direct ionization (DI) of the target molecule (without projectile neutralization) thus yielding branching rations for these two different ionization processes. Results have been compared with recent similar experiments on uracil [Tabet *et al.* unpublished] and water [Gobet *et al.* Phys. Rev. A 70 (2004) 062716]. Although in all cases both processes (EC and DI) produced the same fragment ion groups in the mass spectra, fragmentation is for EC larger than for DI. Moreover the fragmentation ratio for dissociative ionization was observed to be for thymine larger than for adenine, cytosine, and uracil.

Key Words

DNA bases, adenine, cytosine, thymine, uracil, proton impact, ionization, dissociative ionization, electron capture, mass spectrometry

1.   Introduction

Radiation-induced modification of DNA (deoxyribonucleic acid) leading to strand breaks and clustered lesions has long been recognized as a possible origin of mutations and cancers in living systems [von Sonntag 1987]. More recently, a number of specific projectile-molecule interactions have been directly linked to the formation of DNA strand breaks [e.g. Boudaiffa *et al.* 2000]. These results have inspired extensive experimental and theoretical research on irradiation effects in isolated biomolecules (as these targets are much easier to access than liquid or solid samples) with the aim to identify nano-scale processes leading to (multi-)fragmentation events in and around DNA. Although certainly not being directly mirroring processes happening *in vivo* samples, the results obtained for radiative interactions with gas-phase biomolecules have enabled diverse excitation, ionization, and dissociation processes to be observed directly, revealing detail which cannot be extracted from studies of condensed material. In particular, several recent studies have focused on proton collisions with gas-phase DNA bases which may be considered to mimick interactions occurring during *proton therapies* [Coupier *et al.* 2002, Moretto-Capelle and Le Padellec 2006, Le Padellec *et al.* 2008]. In order to deliver localized doses of energy to destroy cells within tumors, these treatments exploit the *Bragg peak* energy for maximum energy deposition by incident protons with kinetic energies of about 100 keV (2.0 v_0 in Bohr velocity units). The occurrence of the Bragg peak results from the interplay between ionization, excitation, and charge exchange processes as the projectiles slow down in the exposed tissue [Biaggi *et al.* 1999, Cabrera-Trujillo *et al.* 2003].

The present investigation is dedicated to proton interaction with the purine molecule adenine ($C_5H_5N_5$), and the pyrimidines cytosine ($C_4H_5N_3O$) and thymine ($C_5H_6N_2O_2$). Adenine and thymine form a Watson-Crick pair in DNA with two hydrogen bonds in the characteristic helical structure. Guanine, which pairs with cytosine via three hydrogen bonds in DNA, was not studied in the present investigation due to the reported difficulty of achieving a sufficiently high vapor pressure without significant isomerization and / or thermal decomposition [Periquet *et al.* 2000]. Infra-red spectroscopy studies of adenine, thymine, and uracil [Colarusso *et al.* 1997] at 200-325℃ indicate that the tautomeric forms shown in Fig. 1 account for >99% of the sublimated molecules (uracil has been included in the present study in order to allow comparison as given in section 3.3). Whereas gas-phase cytosine is thought to be typically present in the keto form, De Vries and co-workers' [2002] invoking REMPI spectroscopic studies of laser-desorbed jet-cooled cytosine provided evidence for a

significant additional population in the enol form characterized by an H atom bonding to the O atom instead of bonding at the N1 position (see Fig.1).

The present work provides the first fragmentation patterns (mass spectra) for the ionization of gas phase DNA base molecules as a function of charge exchange between the projectile and target molecule (i.e.,allowing to distinguish between electron capture processes and direct ionization reactions) at an impact velocity approximately coinciding with maximum energy deposition. To the author's knowledge, the only previous measurements of this kind have been carried on uracil [Tabet et al. unpublished], O_2 [Luna et al. 2005], and H_2O [Gobet et al. 2001, 2004, Luna et al. 2007]. Therefore, in addition to their potential use for nano-scale models of ion-induced radiation damage [Friedland et al. 2003], the present results are of fundamental interest with respect to the production of fragment ions through electron capture and direct ionization in the case of electronically complex target molecules.

2.   Experimental

The crossed-beam apparatus used for the present experiments is shown schematically in Fig. 2 and has been described in detail elsewhere [Gobet et al. 2001, Gobet et al. 2004, Tabet et al. unpublished]. Briefly, protons produced in a standard RF-gas discharge source (80 MHz) were accelerated to 80 keV with an energy resolution ($\Delta E/E$) of 0.01. The *primary* magnetic sector field was used to separate protons from other ions in the source (e.g. H_2^+ and H_3^+), the background pressure was maintained below 10^{-6} Torr along the ensuing beamline. After collimation, the proton beam was crossed at right angles with an effusive target beam of DNA base molecules. This target beam was formed by the sublimation of adenine, cytosine, or thymine powder purchased from Sigma-Aldrich (minimum purity 99%) in a temperature-controlled Knudsen-type oven at 175 – 200 °C. Previous studies indicate that minimal thermal decomposition and isomerization of these nucleobases occurs at these temperatures [Desfrançois et al. 1996]. Accordingly, no evidence was observed for temperature dependence in the present mass spectra. The charge state of the projectile after a collision with a nucleobase molecule was determined using the *secondary* magnetic sector field analyzer with three channeltron detectors located at the corresponding positions to detect H^+, H^0 and H^-.

A costums-built linear time-of-flight (TOF) mass spectrometer was used to analyze the product ions formed by the impact of a proton with a DNA base molecule. The detection of the projectile after

its interaction with a target molecule provided the reference time for the time-of-flight determination of the mass-to-charge ratio of the product ions. By simultaneously determining the mass-per-charge ratio of the product ions and the post-interaction charge of the projectile, the experiment enabled *direct ionization* (product ion detection with coincident H^+ detection after the secondary magnetic analyzer) to be distinguished from *electron capture* (coincident H^0 detection) for each ionizing collision. Thus, in the present terminology, direct ionization (DI) describes the removal of an electron from the nucleobase molecule without projectile neutralization, and electron capture (EC) describes the transfer of an electron from the nucleobase molecule to the projectile. The branching ratios and fragmentation patterns (mass spectra) presented in section 3 correspond to single ion production only; events involving the detection of two or more fragment ions in coincidence with a single projectile are not included here, i.e., due to the relatively poor statistics, this paper does not present results for double ion production events, double electron capture events, and double ionization events involving both projectile neutralization *and* electron emission.

3.   Results and Discussion

3.1.   Branching ratios for electron capture

Ions formed by electron capture in 80 keV collisions with adenine, cytosine, and thymine are expressed as a percentage of the total ion production (summed up EC plus DI production) in table 1. The table also lists EC branching rations derived from recent proton impact experiments on uracil [Tabet *et al.* unpublished] and water [Gobet *et al.* 2004, Shah *et al.* 2007], as well as the appearance energies for the major ions as given in literature. The measured EC branching ratios for adenine, cytosine, thymine, and uracil lie within each other's error limits, as may be expected considering the broadly similar compositions, geometries, and ionization energies of the three molecules. Moreover, the close agreement of the nucleobase results with the water results suggests that the lowest ionization energy is not a decisive factor influencing of the ratio of EC to DI events in 80 keV proton collisions with these molecules. Indeed the intense production of fragment ions shown in figures 3-5 and tables 2-5 (e.g. fragment ion production by EC divided by total ion production by EC being 94% for 80 keV proton impact for thymine) suggests that the removal of electrons from valence orbitals other than the HOMO may contribute significantly to the present data.

3.2. 80 keV proton impact mass spectra

3.2. I. Adenine

Fig. 2 shows the mass spectrum for single ion production by electron capture and direct ionization in collisions between gas-phase adenine molecules and 80 keV (1.8 v_0) protons. *Group 1 through group 8* correspond to the production of fragment ions containing 1-8 of the *heavier atoms* C or N. Although the relative production of fragment ions was different for direct ionization and electron capture (see section 3.3), the same mass peaks were observed for both processes.

The studies of Schlathölter *et al.* [2006A & B] and Brédy *et al.* [2005] on gas-phase adenine provide the only previous measurements of fragment ion production with m/q < 12 Thomson. Schlathölter *et al.* [2006A & B] reported TOF mass spectra for 0.26 v_0 C^+, 0.45 v_0 He^{2+}, 0.47 v_0 C^{5+}, and 0.35 v_0 O^{5+} impact. For single electron capture by incident 0.28 v_0 F^{2+} projectiles, Brédy *et al.* [2005] observed electron emission in coincidence with product cations. The present data shows significant production of H^+ but provides no evidence for ions in the range 2-11 Thomson attributable to H_2^+ or *small* doubly-charged fragments. The only previous singly-charged ion (i.e.with C^+ projectiles) impact mass spectrum covering this m/q range shows weak H_2^+ production but no peaks for doubly-charged ions [Schlathölter *et al.* 2006A]. Conversely, the previous mass spectra for 0.45 v_0 He^{2+} impact [Schlathölter *et al.* 2006A], for 0.47 v_0 C^{5+} [Schlathölter *et al.* 2006B] impact, and for double or triple ionization upon 0.28 v_0 F^{2+} impact [Brédy *et al.* 2005] demonstrate quite significant ion signals between the major peaks at 1 and 12 Thomson. The 0.35 v_0 O^{5+} impact mass spectrum shows quite clear peaks at 2 and 4-8 Thomson [Schlathölter *et al.* 2006A]. The production of doubly charged fragment ions by multiply charged ion impact can be rationalized that greater projectile charge states increase the probability of multiple electron capture. Moreover, the strong fields around multi-charged ions enable electron capture to take place in collisions with relatively large impact parameters (more distant interactions), associated with lower energy transfer [Cabrera-Trujillo *et al.* 2000]. Hence increased H_2^+ production by multi-charged ion impact may be explained by the formation of relatively stable excited parent ions in large-impact-parameter interactions enabling more nuclear rearrangements to occur as the system relaxes prior to fragmentation. It should be noted that electron capture processes dominate in the velocity range studied by Schlathölter *et al.* [2006A & B] and Brédy

et al. [2005] (0.26-0.47 v_0) and that the impact parameters for the presently observed EC interactions at 1.8 v_0 can be assumed to be at least an order of magnitude smaller.

For 0.28 v_0 F^{2+} collisions with gas-phase adenine, Brédy *et al.* [2005] were able to identify the number of electrons emitted from the molecule in single-EC events. A small peak at 18 Thomson, attributable to NH_4^+ fragments or to the ionization of H_2O impurities, was observed in the mass spectrum for single electron capture without electron emission [Brédy *et al.* 2005]. However, no equivalent peak was apparent for single electron capture with the emission of 1, 2, or 3 electrons. In these mass spectra, only *single EC with zero electron emission* can produce peaks at m/q corresponding to the *parent* ion (adenine or an impurity). Therefore, the disappearance of the 18 Thomson peak for electron capture with electron emission [Brédy *et al.* 2005] implies that it was attributable to non-dissociative ionization of H_2O. The low background pressure (10^{-8} mbar) in Brédy *et al.*'s [2005] experiments indicates that any significant impurity must have been due to the target jet. Although heating to 130ºC [Brédy *et al.* 2005] (or up to 200 ºC in the present work) would generally be expected to remove water from the sample prior to measurements, long periods of degassing may be required to remove water trapped within grains of the nucleobase powder (as observed for uracil by Abouaf and Dunet [2005]). In the present work, while background measurements provided no evidence for water, Fig. 2 includes a major peak at 18 Thomson. The relative intensity of the 18 Thomson peak varied significantly for the five separate measurements which were summed up to obtain this mass spectrum. This variation may be attributed to differences in heating times and temperatures leading to more or less effective water removal from the sample prior to the experiments. Therefore, the 18 Thomson peak in Fig. 2 is assigned primarily to H_2O impurities in the sample jet. Similarly, the 17 Thomson peak is assigned to a combination of NH_3^+ production from adenine and OH^+ from H_2O.

In the present measurements, slightly stronger ion production was observed at 12 and 13 Thomson (C^+ and CH^+) than at 14 and 15 Thomson (N^+ and NH^+, although CH_2^+ and CH_3^+ may also contribute). The mass spectrum reported by Schlathölter *et al.* [2006A] for the ionization of gas-phase adenine in 0.26 v_0 collisions with C^+ projectiles also shows larger production of C^+ than N^+. Conversely, Brédy *et al.* [2005] reported negligible C^+ produced but strong N^+ production for single electron capture from adenine without electron emission. As the present results include only single ion production channels, this discrepancy with Brédy *et al.*'s [2005] *zero electron emission* results is quite

surprising. However, it can be rationalized by considering that whereas N^+ can be produced by breaking one C-N and two N-H bonds, or one C-N and one C=N bond, C^+ production involves breaking one double bond (C=C or C=N) and two single bonds (C-C, C-N, or C-H). Therefore, C^+ production is expected to require greater energy transfer, generally associated with smaller impact parameters (more *direct* collisions). Accordingly, increased relative C^+ production was observed by Brédy *et al.* [2005] for electron capture with single, double, and triple electron emission, corresponding to interactions with successively smaller impact parameters. As the impact parameters for single electron capture without electron emission are much larger in Brédy *et al.*'s [2005] slow (0.28 v_0) doubly-charged ion impact experiments than in the relatively fast (1.8 v_0) proton-molecule collisions studied in the present work, this then explains nicely the observed discrepancy.

For product ions ≥ 20 Thomson, in addition to the experiments of Brédy *et al.* [2005] and Schlathölter *et al.* [2006A & B], Avarado *et al.* [2007] have recently reported mass spectra for 0.75 v_0 H^+, 0.37 v_0 He^+, and 0.22 v_0 C^+ impact on gas-phase adenine. These results may be compared to similar measurements with neutral projectiles (H^0, He^0, and C^0) [Avarado *et al.* 2007]. The same main nine groups of product ions were observed in both the present study and in the previous one. However, whereas *groups 7* and *9* are weak but visible in Schlathölter *et al.*'s [2006A] 0.26 v_0 C^+ impact result and in Jochims *et al.*'s [2005] 20 eV photo-ionization mass spectrum, they are not discernable in Fig. 2 (although table 5 shows that ion production in *group 7* was marginally higher than the background noise) or in the data of Avarado *et al.* [2007], Brédy *et al.* [2005], and Schlathölter *et al.* [2006B]. The weak production of fragment ions >115 Thomson is consistent with the conjecture of Leach and co-workers' [Jochims *et al.* 2005, Schwell *et al.* 2006] proposal that fragmentation following photo-ionization originates from metastable (adenine$^+$)* with the positive charge (*hole*) localized on the NH_2 group. Accordingly, NH_2^+ production is expected to dominate single ionization involving the removal of one C or N but leaving the *double ring* structure intact, while the removal of an atom from within the double ring will generally cause multi-fragmentation.

The group maxima observed by Schlathölter *et al.* [2006A] are consistent with the present data, while minor differences in peak positions of the heavier fragment ions may be due to the relatively low resolution of the present data. Table 2 compares the ion masses observed in the present work with those reported by Rice *et al.* [1967] for 70 eV (2.3 v_0) electron impact and by Jochims *et al.* [2005] for 20 eV photo-ionization. The assignments proposed by the previous authors are generally

consistent, with the exception of the peak at 53 Thomson, which was attributed to $C_3H_3N^+$ and $C_2HN_2^+$ by Brédy *et al.* [2005] and Jochims *et al.* [2005], respectively. The principle pathway identified in the literature is based around the sequential loss of HCN groups, while electron impact studies of variously labeled adenine derivatives [Occolowitz 1968, Barrio *et al.* 1981, Sethi *et al.* 1982] suggest that dissociation along the C(2)-N(3) and N(1)-C(6) bonds dominates (see Fig. 1). The work of Jochims *et al.* [2005] provides a thorough review of adenine fragmentation pathways and predicts significant bond rearrangements in the key metastable cations prior to fragmentation.

Moreover, Alvarado *et al.* [2007] observed clear evidence for the production of adenine^{2+} (67.5 Thomson) in all of their ion and neutral impact studies. This demonstrates an unusually high stability of the doubly charged adenine ion and leads us to expect its production to contribute to the present results. However, the mass resolution of the present spectrum is insufficient to separate evidence for adenine^{2+} from ion production at 67 and 68 Thomson, also clearly observed by Alvarado *et al.* [2007].

Alvarado *et al.*'s [2007] high TOF resolution data also revealed shifts in peak positions away from integer values of m/q which were attributed to sequential fragmentation events occurring in the field-free region between the extraction and reflectron parts of the mass spectrometer. Although it was not possible to observe these effects in the present lower-resolution linear TOF experiments, Alvarado *et al.*'s [2007] analysis highlights that the stability of excited ionic states may lead to significant differences between different adenine mass spectrometry experiments. In particular, the high energy deposition expected under the present ionizing conditions is expected to lead to (adenine$^+$)* production in highly excited states and thus the observation of only a few *parent* and large fragment ions (see section 3.3).

3.2. II. Cytosine

The mass spectra for single ion production through electron capture and direct ionization in 80 keV proton collisions with gas phase cytosine molecules is shown in Fig. 4. The same peak positions were observed for both ionizing processes.

To the authors' knowledge, the only previous cytosine fragment ion measurements available in the literature were reported for 12 and 70 eV electron impact [Rice *et al.* 1965, NIST] and for 100 keV proton impact [Le Padellec *et al.* 2008]. In addition, ion and cluster ion production has been studied in 10 and 13 eV electron interactions with supersonic jets comprising cytosine and a carrier

gas (He, Ar, H_2O, or a mixture of these gases) [Kim *et al.* 1996]. Kim *et al.* [1996] reported that the strongest peaks corresponded to multiples of 109 Thomson and interpreted this result as providing evidence that cytosine loses two hydrogen atoms upon *modest heating* [Kim *et al.* 1996]. Conversely, the present results show a local maximum at 111 Thomson and no clear evidence for ion production at 109 Thomson, in agreement with the previous mass spectra for gas-phase cytosine [Rice *et al.* 1965, NIST, Le Padellec *et al.* 2008]. Furthermore, the intensity of the peak at 112 Thomson in Rice *et al.*'s [1965] high-resolution mass spectrum was ~10% of the peak at 111 Thomson, consistent with the molecular weight of 111.10 listed in the NIST database [NIST]. This strongly suggests that uracil *impurities* or protonated cytosine do not contribute significantly to the present data. We suspect that the relatively complex peak structure between 108 and 113 Thomson in Kim *et al.*'s [1966] electron impact mass spectrum was due to the ionization and subsequent break-up of clusters containing cytosine molecules, as opposed to heating effects on monomers. This rationale also implies that the target jet for the present experiments did not contain a significant density of cytosine dimers or larger clusters.

The mass spectra generated using high-energy (>> IE) electron impact by Rice *et al.* 1965, NIST and the 100 keV proton impact on cytosine [Le Padellec *et al.* 2008] show the same major groups of product ions as observed in the present data. The peak positions observed in the present and previous mass spectra are listed in table 3 [Rice *et al.* 1965, Le Padellec *et al.* 2008] and the proposed assignments are broadly consistent with Rice *et al.*'s [1965] discussion of dissociative ionization pathways. Whereas *groups 7* and *9* were absent in some of the adenine data, all possible groups (0-8) are clearly present in the cytosine mass spectrum. The strong production of large fragment ions implies that a significant proportion of dissociative ionization events originate from a (cytosine$^+$)* ion with the positive charge (hole) localized on the central C_4N_2 ring. This is consistent with Jochims *et al.*'s [2005] association of uracil and thymine dissociative ionization with metastable precursors characterized by hole localization on the N(1) atom (Fig. 1). Accordingly, Rice *et al.* [1965] suggested the removal of the neutral amino group (NH_2) as the first step in one of three major fragmentation pathways for ionized cytosine, thus accounting for the peak at 93 Thomson. The next step in this proposed pathway is the expulsion of HCN, associated with the 68 Thomson peak.

The second pathway proposed by Rice *et al.* [1965] for the dissociative ionization of cytosine begins with CO expulsion (accounting for the peak at 83 Thomson) followed by HCN loss (leaving an

ion of 56 Thomson). Retro *Diels-Alder* reactions were suggested [Rice *et al.* 1965] as the third main pathway beginning with the expulsion of NCO or HNCO, possibly preceded by H loss (leaving ions of 67-69 Thomson). The next step is HCN expulsion, corresponding to ion production at 40-42 Thomson. The presently observed difference of 27 Thomson (HCN) between the local maxima of these groups (68 and 41 Thomson) appears to be consistent with this proposed sequence.

Whereas only the lowest ionization energy of cytosine has been measured directly (8.45 eV [Dougherty *et al.* 1978], table 1), an indication of fragment ion appearance energies is provided by Rice *et al.*'s [1965] 12 eV electron impact mass spectrum which shows peaks at 68, 69, 83, 84 (very weak), 111, and 112 Thomson. The only peaks in the photo-ionization mass spectra of thymine and uracil [Jochims *et al.* 2005] which had appearance energies below 12 eV by more than a few tenths of an eV (see table 1) occurred at 83 and 69 Thomson, respectively. The 83 Thomson peak in the thymine spectrum was assigned to $C_4H_5NO^+$ production [Jochims *et al.* 2005] which for cytosine would require significant atomic rearrangement prior to fragmentation or the removal of the double-bonded N(3) atom from the ring (see Fig. 1). Therefore, Rice *et al.*'s [1965] $C_3H_5N_3^+$ assignment (CO loss) seems the most probable for the 83 Thomson peak in the cytosine mass spectrum, although $C_2HN_3O^+$ production via the cleavage of the N(1)-C(6), the C(4)-C(5), and two N-H single bonds may also be contributing. At 69 Thomson, Jochims *et al.*'s [2005] assignment of the peak in the uracil mass spectrum to $C_3H_3NO^+$ production represents a plausible alternative to Rice *et al.*'s [1965] $C_3H_5N_2^+$ (NCO loss) proposal for the corresponding peak in the cytosine data. $C_3H_3NO^+$ can be formed from both cytosine and uracil without any atomic rearrangement or double bond breaking prior to dissociation.

The only previous fragment ion assignments below the major peak centered at 41 Thomson in the cytosine mass spectrum have been proposed by Le Padellec *et al.* [2008] for 100 keV proton impact ionization (C^+, CH^+, N^+, NH^+ and OH^+ in *group 1*, and CH_2N^+ or CO^+ for the peak at 28 Thomson). The present assignments are based primarily on analogies with the other nucleobases. All three DNA bases discussed here and uracil [Tabet *et al.* unpublished] feature strong peaks at 28 Thomson. It is also worth noting that the appearance energies for the 28 Thomson ions (not measured for cytosine) are close to each other,i.e., for adenine 13.1 ± 0.1 eV, thymine 13.6 ± 0.1 eV, and uracil 13.75 ± 0.05 eV [Jochims *et al.* 2005]. These similar appearance energies suggest that this mass peak may be associated with similar fragment ions for these nucleobases. As oxygen is not present in

adenine, this implies that CO$^+$ and COH$^+$ product ions may contribute relatively weakly to the peak centered at 28 Thomson in the cytosine mass spectrum. This appears to be consistent with the major role of HCN expulsion in Rice *et al.*'s [1965] description of sequential fragmentation following cytosine ionization and with the expected localization of the metastable cytosine cation's positive charge (hole) on the N(1) atom. However, electron impact ionization experiments on deuterated thymine in the gas phase [Imhoff *et al.* 2005] indicate that CO$^+$ may also contribute to the thymine mass spectrum. Accordingly we assign the cytosine *group 2* primarily to CNH$_n^+$ (*n* = 1-3) production, in general agreement with Jochims *et al.*'s [2005] assignments for 20 eV photo-ionization of gas phase uracil and thymine, with weaker contributions from CO$^+$ and C$_2$H$_n^+$.

In the 10-20 Thomson range of the present cytosine mass spectrum, the strong peak at 16 Thomson may be rationalized in terms of the relative ease of breaking the single N-C(4) bond between the central ring and the amino group (NH$_2$). The production of 18 Thomson ions is weak in comparison with the mass spectrum reported by NIST [NIST]. This suggests that the peak may be primarily due to water impurities whose levels can be expected to vary for different measurements.

To the authors' knowledge, the present work provides the first demonstration in the literature of H$^+$ fragment ion production from gas-phase cytosine. No clear evidence is observed for the formation of H$_2^+$ ions or any doubly charged fragments in the range from 2-11 Thomson.

3.2. III. Thymine

Fig. 5 shows the mass spectrum for single ion production by EC and DI in 80 keV (1.8 v_0) proton collisions with gas-phase thymine. In common with the equivalent results for adenine, cytosine, and uracil [Tabet *et al.* unpublished], the same peaks were observed for electron capture and for direct ionization in the present collisions.

In contrast with cytosine, a number of previous experimental studies have been carried out on the ion impact induced ionization of thymine. In particular, Le Padellec *et al.* [2008] have measured ion production following 100 keV proton impact, while Schlathölter and co-workers have presented TOF mass spectra for gas-phase thymine ionized with incident 0.4 v_0 C^{5+} [Schlathölter *et al.* 2006B], 0.5 v_0 O^{5+} [Schlathölter *et al.* 2006 B], 0.3 v_0 C$^+$ [Schlathölter *et al.* 2005, de Vries *et al.* 2004], 0.2 v_0 Xe^{8+} [Schlathölter *et al.* 2006 A], 0.2 v_0 Xe^{25+} [de Vries *et al.* 2004], 0.4 v_0 Xe^{25+} [Schlathölter *et al.* 2004], and 0.4 v_0 C^{3+} and C^{6+} [de Vries *et al.* 2004]. Fig. 5 and the previous ion impact mass spectra provide

evidence for ion production within all the possible groups (1-8), although *groups 7 and 8* (with respective maxima at 98 and 112 Thomson in the present data) were generally observed to be weak.

De Vries *et al.* [2004] commented that the production of thymine fragment ions with m/q larger than that of the singly-ionized C_4N_2 ring (74 Thomson) implies dissociative ionization without the destruction of the ring itself. We agree that the weak 108-115 Thomson band observed in the present result with a maximum at 112 Thomson points to fragmentation around the CH_3 group, notably CH_2 removal with a minor nuclear arrangement to form uracil$^+$. Indeed, the net positive charge remaining with the larger fragment in this process is consistent with Jochims *et al.*'s [2005] description of the (thymine$^+$)* precursor with hole localization on the N(1) atom. Although neither Jochims *et al.* [2005] nor Rice *et al.* [1965] reported ion production in this m / q range in their respective 20 eV photo-ionization and 70 eV (2.3 v_0) electron impact experiments, respectively, a weak peak is apparent at 112 Thomson in Imhoff *et al.'s* [2005] 70 eV electron impact mass spectrum of gas phase thymine.

The 95-100 Thomson group observed in the present work with a maximum at 98 Thomson (97 Thomson in the previous high-resolution electron impact and photo-ionization experiments [Jochims *et al.* 2005, Rice *et al.* 1965, Imhoff *et al.* 2005]) was tentatively associated with CH_2N removal by Jochims *et al.* [2005], presumably following cleavage of the C(2)-N(1) and C(6)-C(5) single bonds of metastable (thymine$^+$)*. The weakness of the peak may be partially explained by hole localization on the N(1) atom of (thymine$^+$)* tending to leave the larger fragment neutral. This proposal appears to be consistent with the strong peak at 28 Thomson, although direct CH_2N^+ loss from (thymine$^+$)* has not been identified as a major reaction pathway in previous studies [Jochims *et al.* 2005, Rice *et al.* 1965, Imhoff *et al.* 2005].

Jochims *et al.* [2005] associated the relatively strong *group 6* with the loss of HCNO following the rupture of the N(1)-C(2) and N(3)-C(4) bonds which are single in both thymine and (thymine$^+$)*. This assignment was supported by Imhoff *et al.*'s [2005] analysis of thymine-methyl-d_3-6-d (CH_3 and CH in thymine replaced with CD_3 and CD, respectively) ionization by 70 eV electrons. The local maximum at 83 Thomson in the 20 eV photo-ionization and 70 eV electron impact mass spectra [Jochims *et al.* 2005, Rice *et al.* 1965, Imhoff *et al.* 2005] is presumably due to the lower appearance energy of $C_4H_5NO^+$ (10.7 eV) than $C_4H_4NO^+$ (13.2 eV). Conversely, the group maximum at 82 Thomson in Fig. 5 suggests that $C_4H_5NO^+$, identified by Jochims *et al.* [2005] as an intermediate state

in a number of key reaction pathways, may be relatively short-lived in the present proton impact experiments due to the tendency for higher energy deposition.

The *group 7* maximum was observed at 70 Thomson in the present experiments and in the previous 70 eV electron impact data [Rice *et al.* 1965, Imhoff *et al.* 2005], whereas the local maximum for 20 eV photo-ionization maximum was reported at 71 eV [Jochims *et al.* 2005]. Jochims *et al.*'s [2005] assignment of the respective peaks to $C_2HNO_2^+$ and $C_2H_2N_2O^+$ with entirely separate reaction pathways appears to be consistent with the relative intensities varying according to the ionizing interaction. The group was not observed at all in Rice *et al.*'s [1965] 20 eV electron impact result.

The peak structure between 20 and 60 Thomson (*groups 2-4*) in Fig. 5 is generally consistent with the previous ion impact [e.g. De Vries *et al.* 2004], 70 eV electron impact [Rice *et al.* 1965, Imhoff *et al.* 2005] and 20 eV photo-ionization mass spectra [Jochims *et al.* 2005]. The work of Jochims *et al.* [2005] provides a thorough review of the fragmentation pathways. The only apparent discrepancies between the present and previous studies in this m/q range [Rice *et al.* 1965, Imhoff *et al.* 2005, Jochims *et al.* 2005] relate to *group 3* (37-45 in the present work). In particular, whereas we observed a local maximum at 43 Thomson, the previous results demonstrated increased ion production at 44 Thomson [Rice *et al.* 1965, Imhoff *et al.* 2005, Jochims *et al.* 2005]. These peaks have been assigned to $HCNO^+$ [Imhoff *et al.* 2005, Jochims *et al.* 2005, De Vries *et al.* 2004], H_2CNO^+ [Imhoff *et al.* 2005], and to CO_2^+ due to an impurity in the beam [Jochims *et al.* 2005].

Whereas the 80 keV (present work) and 100 keV [Le Padellec *et al.* 2008] proton impact data show the local maximum at 43 Thomson to be more intense than its 39 Thomson counterpart, the opposite relation was observed for 70 eV electron impact [Imhoff *et al.* 2005] and 0.28-0.45 v_0 C^{n+} (n = 1 and 3) impact [Schlathölter *et al.* 2005, de Vries *et al.* 2004] (the situation in the photo-ionization experiments is unclear due to a CO_2 impurity). $HCNO^+$ production (43 Thomson) has been attributed to a charge reversal in the fragmentation associated with *group 6*, identified by Jochims *et al.* [2005] as the first step in the most important pathways for sequential fragmentation following ionization. This presumably occurs primarily through the cleavage of the C(2)-N(3) and C(4)-C(5) bonds, tending to leave the larger fragment charged due to hole localization on the N(1) atom in the metastable (thymine$^+$)* precursor. Conversely, breaking the (thymine$^+$)* bonds C(2)-N(3) and N(1)=C(6) (single bonded in neutral thymine) would tend to produce $HCNO^+$. As cleaving the N(1)=C(6) double bond will require greater energy transfer, the latter pathway is expected to be relatively probable in the present

collisions. By contrast, $C_3H_3^+$ (39 Thomson) production occurs via a sequence of 3 fragmentations with considerable atomic scrambling. Therefore we propose that this channel may be supressed in the present measurements compared to the 70 eV electron impact data [Imhoff *et al.* 2005] due to the tendency for more rapid fragmentation following high energy deposition. Comparisons with De Vries *et al.*'s [2004] C^{n+} (*n* = 1, 3, and 6) impact data are complicated by interactions with the projectiles' bound electrons. Stronger peaks of 43 and 44 Thomson than at 39 Thomson in the previous highly charged ion impact mass spectra (C^{5+}, C^{6+}, O^{6+}, Xe^{8+}, and Xe^{25+}) [Schlathölter *et al.* 2004, Schlathölter *et al.* 2006 A, Schlathölter *et al.* 2006 B, de Vries *et al.* 2004] can be rationalized in terms of relatively large cross sections for multi-ionization and the significant production of (43, 82) and (44, 82) Thomson ion pairs observed in de Vries *et al.*'s [2004] coincidence experiments.

As mentioned in section 3.2.II, Imhoff *et al.*'s [2005] electron impact ionization experiments on deuterated thymine provided evidence that CO^+ (28 Thomson) production from gas-phase thymine is not negligible. Accordingly, while the intense *group 2* is mainly associated with CNH_n^+ (*n* = 1-3) ions following Jochims *et al.*'s [2005] analysis, CO^+ and $C_2H_n^+$ (*n* = 1- 3) product ions are also expected to contribute to the 80 keV proton impact mass spectrum shown in Fig. 5.

The present thymine mass spectrum includes a distinct yet fairly weak peak at 18 Thomson, whereas Imhoff *et al.* [2005] observed the group maximum at this m/q for 70 eV electron impact ionization. The relatively slow ion impact measurements of Schlathölter and co-workers [de Vries *et al.* 2004, Schlathölter *et al.* 2005, Schlathölter *et al.* 2006 B] also showed strong ion production at 18 Thomson. To clarify assignments, Imhoff *et al.* [2005] carried out complimentary experiments on gas-phase thymine-methyl-d_3-6-d (CH_3 and CH in thymine replaced with CD_3 and CD, respectively). In this case the local maximum was observed at 18 Thomson, attributable to CD_3^+ and / or H_2O^+ ions. The authors also observed a peak at 20 Thomson, strongly suggesting the formation of D_2O^+ product ions. By analogy, it is probable that the present 18 Thomson peak contains a contribution of H_2O^+ product ions from (thymine$^+$)* dissociation. The difference in the relative intensity of the 18 Thomson peak between the present and previous data may be due to changes in the relative contributions of different fragmentation pathways according to the collision conditions and / or to different levels of H_2O impurities in the target beams.

Ion production in the range of 10-20 Thomson following 80 keV proton impact upon thymine shows a local maximum at 15 Thomson. This is consistent with the relatively low energy required to

break the single C-C bond joining the CH_3 group to the C_4N_2 ring. Accordingly, Imhoff *et al.*'s [2005] 70 eV electron impact experiments showed the 15 Thomson peak to be the most intense in *group 1*, with the exception of the 18 Thomson peak discussed above. Conversely, Schlathölter and co-workers' C^{n+} and O^{5+} impact experiments on gas phase thymine consistently showed the production of C^+ (as well as H_2O^+) to be much stronger than any other ion in the group [de Vries *et al.* 2004, Schlathölter *et al.* 2006 B]. Particularly in the case of multi-charged ion impact, this discrepancy with the present work may be partially due to double or multiple fragment ion production in single collision events (not counted in the present data). Furthermore, the electronic structure of the projectile has been identified to play a major role in the ionization dynamics of thymine and uracil [Schlathölter *et al.* 2005].

Unlike the results for adenine, cytosine, and uracil [Tabet et *al.* unpublished], the present work reveals clear evidence for ion production at 2 Thomson from gas phase thymine. Strong H_2^+ production is also visible in each of Schlathölter and co-workers' ion impact mass spectra [e.g. de Vries *et al.* 2004] and in Imhoff *et al.*'s 70 eV electron impact data [2005]. Additional peaks at 3 and 4 Thomson in Imhoff *et al.'s* [2005] mass spectrum for thymine-methyl-d_3-6-d imply the presence of several competing pathways for H_2^+ production from ionized thymine. Relatively high H_2^+ production may be related to the abundance of C-H bonds (4 in thymine compared to 2 in adenine, cytosine, and uracil), which are weaker than the N-H bonds (see Shukla and Mishra's [1999] optimized bond length calculations for nucleobases). Similarly, table 5 shows the production of H^+ as a percentage of total ionization to be highest for thymine. However, the thymine-methyl-d_3-6-d mass spectrum [Imhoff *et al.* 2005] indicates that the hydrogen atoms from N-H bonds also contribute significantly to H^+ and H_2^+ production from thymine. The analyses of nucleobase dissociative ionization pathways initiated by Rice *et al.* [1965, 1967] and recently reviewed and developed by Jochims *et al.* [2005] do not extend to the formation of fragment ions < 26 Thomson.

3.3. Fragmentation ratios for direct ionization and electron capture

The present experiments enabled direct ionization to be compared with electron capture processes in terms of the fragmentation ratios for ion production in a given m/q range against total ionization. Table 5 shows these fragmentation ratios calculated separately for EC and DI (e.g. the number of product ions in a given m/q range produced by EC divided by the total number of product ions produced by EC). The error bars are purely statistical ($n^{-\frac{1}{2}}$) and do not take into account the mass

spectrometer transmission for different ions. The contribution of background noise could be removed easily as it was observed to be constant for all flight times.

Whereas an incident proton can transfer any amount of its kinetic energy in a single ionizing collision with a molecule (EC or DI), the statistical distribution of ions produced in a large sample of collisions is expected to reflect the specific shape of energy deposition function corresponding to the nature of the interaction. Naturally, the energy transfer threshold for the production of the *parent ion* is lower than that for dissociative ionization. Therefore, increased fragmentation and greater relative production of small fragment ions (see Jochims *et al.*'s [2005] adenine, thymine, and uracil photo-ionization appearance energy results (table 1)) provide evidence for a shift towards higher energy deposition. However, it should be noted that deposited energy can also be disposed of by the molecular system by photon emission or in the form of the KE of an emitted electron, neither of which were detected in the present experiments.

For all four nucleobases in table 5, the production of parent ions (as given in percent of the total ion production) is markedly greater for DI than for EC. This increased tendency for fragmentation following electron capture as compared to direct ionization in 80 keV proton-molecule collisions has been observed previously also for water target [Gobet *et al.* 2001, 2004] and is consistent with the occurrence of small impact parameters where more energy is transfered. Indeed, table 1 demonstrates that the probabilities, that is the cross sections, (and therefore impact parameters) for EC are distinctly smaller than for DI in the present collisions.

As well as demonstrating that the relative contribution of dissociative ionization is greater for EC than DI, table 5 shows which mass ranges account for the addotional fragment ions produced by EC. For all four nucleobases studied here, relative production of H^+ and of ions in *groups 2 and 3*[*] is greater for EC than DI. For *groups 4 to 8*, relative ion production is either greater for DI than EC or about the same. Therefore the increase in dissociative ionization / total ionization for EC compared with DI is principally associated with the production of *small* or *intermediate* fragment ions (m/q < 47), consistent with the occurrence of larger energy deposition in the EC reactions.

It is interesting to consider these results in the context of Alvarado *et al.*'s [2007] comparisons of parent and fragment ion production following singly-charged ion and neutral collisions with gas-phase adenine in the velocity range 0.22-0.75 v_0. For ion impact in this velocity regime, ionization

---

[*] Ion production in *group 1* should be considered with caution due to suspected water impurities.

occurs dominantly by electron capture, whereas electron capture is very weak for neutral impact at all impact velocities. Moreover, for 0.89-2.45 v_0 collisions with water molecules, the cross sections for direct ionization by proton impact were observed to be similar to the total ionization cross sections for neutral hydrogen impact [Gobet *et al.* 2001, 2004, 2006]. Therefore, it is reasonable to draw an approximate analogy between Alvarado *et al.*'s [2007] ion / neutral impact ionization comparisons and the present EC / DI comparisons. As the cross sections (and therefore impact parameters) for electron capture are much larger than those for direct ionization at *low* impact velocities, we would have expected a clear increase in the relative production of fragment ions following neutral impact (analogous to DI) i.e. the opposite trend to the present results. Conversely, Alvarado *et al.* [2007] observed almost no differences in the branching ratios for fragment ion production following H^+ and H^0 impact. This result highlights the potential limitations of the simple association of smaller impact parameters with increased energy deposition as a means to rationalize the ionization-induced fragmentation patterns of electronically complex molecules.

Table 5 shows almost no difference in measured parent ion probabilities (given in percentage of the total ion produced, i.e. fragmentation ratio) in 80 keV (1.8 v_0) collisions with adenine, cytosine, and uracil [Tabet *et al.* unpublished]. Thus, despite the differences in the (nucleobase$^+$)* relaxation pathways discussed in section 3.2 and reflected in the relative intensities of the fragment ion groups in table 5, the overall tendency for the fragmentation of these three molecules is similar under the present ionizing collisions. Only thymine showed distinctly larger fragmentation branching ratios for dissociative ionization / total ionization. The reason for the relative instability of (thymine$^+$)* formed in the present collisions is unclear. However, a simple comparison of the molecular geometries (Fig. 1) suggests that it may be associated with the availability of (thymine$^+$)* relaxation channels involving the initial removal of the CH_3 group. Indeed, while the fragmentation of (uracil$^+$)*, (cytosine$^+$)*, and (thymine$^+$)* is understood to proceed dominantly through initial HNCO loss [Rice *et al* 1966, Jochims *et al.* 2005], the detection of ions in *groups 7 and 8* demonstrates the contribution of further dissociative ionization pathways. Schlathölter *et al.* [2005] also reported greater relative production of fragment ions for thymine than for uracil following 0.28 v_0 C^+ impact.

4.   Conclusions

For single ion production following proton impact upon gas-phase adenine, cytosine, and thymine, branching ratios for electron capture / total ionization (direct ionization + electron capture) have been measured for the first time and agree closely with previous data for 80 keV (1.8 v_0) proton collisions with uracil [Tabet *et al.* unpublished] and water [Gobet *et al.* 2001, 2004, Shah *et al.* 2007]. Separate mass spectra have been recorded for direct ionization and electron capture for each of the DNA bases studied. The two ionization processes produced the same groups of ions, albeit with different relative intensities. The observed product ions were generally consistent with previous measurements, notably for singly-charged ion impact ionization [e.g. Le Padellec *et al.* 2008], 70 eV electron impact ionization [e.g. Imhoff *et al.* 2005], and 20 eV photo-ionization [Jochims *et al.* 2005]. Several differences with previous mass spectra, e.g. a stronger production of $HCNO^+$ than $C_3H_3^+$ in 80 keV proton collisions for thymine as compared to the opposite following 70 eV electron impact [Imhoff *et al.* 2005], can be rationalized on the basis of particularly high energy deposition in the present collisions.

As observed for uracil [Tabet *et al.* unpublished] and water [Gobet *et al.* 2004], the present fragmentation ratios (fragment ion production divided by total ionization) in 80 keV proton collisions with adenine, cytosine, and thymine are greater following electron capture than direct ionization reactions. This ionization process dependence of DNA base fragmentation patterns highlights the necessity of quantitative experimental measurements (notably fragmentation and branching ratios and absolute cross sections) following projectile collisions with biomolecules in order to model radiation damage on the molecular scale.

Acknowledgements

References

R. Abouaf and H. Dunet, *Eur. Phys. J. D* **35** (2005) 405

F. Alvarado, S. Bari, R. Hoekstra, and T. Schlathölter. *J. Chem. Phys.* **127** (2007) 034301

M. G. Barrio, D. I. C. Scopes, J. B. Holtwick, and N. J. Leonard, *Proc. Natl. Acad., Sci.*, USA **78** (1981) 3986

M. Biaggi, F. Ballarini, W. Burkard, E. Egger, A. Ferrari, A. Ottolenghi, *Nucl. Instr. Methods Phys. Res. B* 159 (1999) 89

B. Boudaiffa, P. Cloutier, D. Hunting, M.A. Hues, and L. Sanche, Science **287** (2000) 1658

R. Brédy, J. Bernard, L. Chen, B. Wei, A. Salmoun, T. Bouchama, M. C. Buchet-Poulizac, S. Martin, *Nucl. Instr. and Meth. in Phys. Res. B* **235** (2005) 392

R. Cabrera-Trujillo, Y. Öhrn, E. Deumens, and J. R. Sabin, *Phys. Rev. A* **62** (2000) 052714

R. Cabrera-Trujillo, P. Apell, J. Oddershede, and J. R. Sabin, *Application of Accelerators in Research and Industry International Conference: AIP Conference Proceedings* **680** (2003) 86

M. Carré, M. Druetta, M. L. Gaillard, H. H. Bukow, M. Horani, A.L. Roche, and M. Velghe, *Mol. Phys.* **40** (1980) 1453

P. Colarusso, K. Zhang, B. Guo, and P. F. Bernath, *Chem Phys. Lett.* **269** (1997) 39

B. Coupier, B. Farizon, M. Farizon, M. J. Gaillard, F. Gobet, N. V. de Castro Faria, G. Jalbert, S. Ouaskit, M. Carré, B. Gstir, G. Hanel, S. Denifl, L. Feketeova, P. Scheier, and T. D. Märk, *Eur. Phys. J. D* **20** (2002) 459

J. de Vries, R. Hoekstra, R. Morgenstern, and T. Schlathölter, *J. Phys. B: At. Mol. Opt. Phys.* **35** (2002) 4373

J. de Vries, R. Hoekstra, R. Morgenstern, and T. Schlathölter, *Physica Scripta* **T110** (2004) 336

C. Desfrançois, H. Abdoul-Carime, and J. P. Schermann, *J. Chem. Phys.* **104** (1996) 7792

W. Friedland, P. Jacob, P. Bernhardt, H. G. Paretzke, and M. Dingfelder, *Radiat. Res.* 159 (2003) 401

F. Gobet, B. Farizon, M. Farizon, M.J. Gaillard, M. Carre, M. Lezius, P. Scheier, and T.D. Märk, *Phys. Rev. Lett.* **86** (2001) 3751

F. Gobet, S. Eden, B. Coupier, J. Tabet, B. Farizon, M. Farizon, M. J. Gaillard, M. Carré, S. Ouaskit, T. D. Märk, and P. Scheier, *Phys. Rev. A* **70** (2004) 062716

F. Gobet, S. Eden, B. Coupier, J. Tabet, B. Farizon, M. Farizon, M. J. Gaillard, S. Ouaskit, M. Carré, and T. D. Märk, *Chem. Phys. Lett.* **421** (2006) 68

M. Imhoff, Z. Deng, and M. Huels, *Int. J. Mass Spectrom.* **245** (2005) 68

H.-W. Jochims, M. Schwell, H. Baumgärtel, and S. Leach, *Chem. Phys.* **314** (2005) 263

S. K. Kim, W. Lee, and D. R. Herschbach, *J. Phys. Chem.* **100** (1996) 7933

D. Lafaivre and P. Marmet, *Can. J. Phys.* **56** (1978) 1549

A. Le Padellec, P. Moretto-Capelle, M. Richard-Viard, J. P. Champeaux, and P. Cafarelli, *Journal of Physics: Conference Series* **101** (2008) 012007

P. Moretto-Capelle and A. Le Padellec, *Phys. Rev. A* **74** (2006) 062705

J. D. Morrison and J. C. Traeger, *Int. J. Mass Sprectrom. Ion Phys.* **11** (1973) 77

E. Nir, M. Müller, L. I. Grace, and M. S. de Vries, *Chem Phys. Lett.* **355** (2002) 59

NIST Chemistry WebBook. Available from http://webbook.nist.gov/

J. L. Occolowitz, *Chem. Commun.* (1968) 1226

V. Periquet, A. Moreau, S. Carles, J. P. Schermann, and C. Desfrançois, *Journal of Electron Spectroscopy and Related Phenomena* **106** (2000) 141

J. M. Rice, G. O. Dudek, and M. Barber, *J. Am. Chem. Soc.* **87** (1965) 4569

J. M. Rice and G. O. Dudek, *J. Am. Chem. Soc.* **89** (1967) 2719

T. Schlathölter, F. Alvarado, and R. Hoekstra, *Nucl. Instr. and Meth. in Phys. Res. B* **223** (2005) 62

T. Schlathölter, F. Alvarado, S. Bari, and R. Hoekstra, *Physica Scripta* **73** (2006) C113 **A**

T. Schlathölter, F. Alvarado, S. Bari, A. Lecointre, R. Hoekstra, V. Bernigaud, B. Manil, J. Rangama, and B. Huber, *ChemPhysChem* **7** (2006) 2339 **B**

T. Schlathölter, R. Hoekstra, R. Morgenstern, *Int. J. Mass Spectrom.* **233** (2004) 173

M. Schwell, H.-W. Jochims, H. Baumgartel, F. Dulieu, and S. Leach, *Planetary and Space Science* **54** (2006) 1073

S. K. Sethi, S. P. Gupta, E. E. Jenkins, C. W. Whitehead, L. B. Townsend, J. A. McCloskey, *J. Am. Chem. Soc.* **104** (1982) 3349

O. V. Shishkin, L. Gorb, A.V. Luzanov, M. Elstner, S. Suhai, and J. Leszczynski, *J. Mol. Structure* **625** (2003) 295

M. K. Shukla and P. C. Mishra, *Chem. Phys.* **240** (1999) 319

C. von Sonntag, *The Chemical Basis for Radiation Biology*, Taylor and Francis, London, 1987

J. Tabet, S. Eden, S. Feil, H. Abdoul-Carime, B. Farizon, M. Farizon, S. Ouaskit, and T. D. Märk, *unpublished*

Fig. 1: Ground-state geometries of the dominant tautomeric forms of gas-phase adenine, thymine, uracil, and cytosine [Colarusso *et al.* 1997, Nir *et al.* 2002]

Adenine (amine)

Thymine (keto)

Uracil (keto)

Cytosine (enol)

Cytosine (keto)
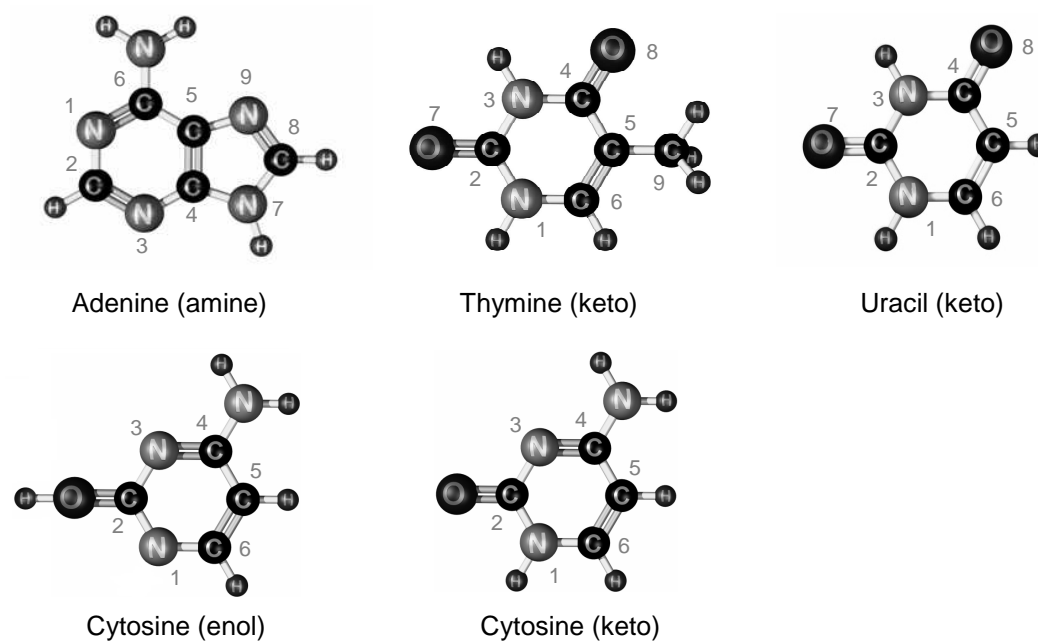
Fig. 2: Schematic diagram of the experimental system

Fig. 3: Mass spectrum for proton impact ionization of adenine ($C_5H_5N_5$, 135 amu) by electron capture and by direct ionization at 80 keV. The main ions expected to account for the peaks are listed in table 2.

Fig. 4: Mass spectrum for proton impact ionization of cytosine ($C_4H_5N_3O$, 111 amu) by electron capture and by direct ionization at 80 keV. The main ions expected to account for the peaks are listed in table 3.
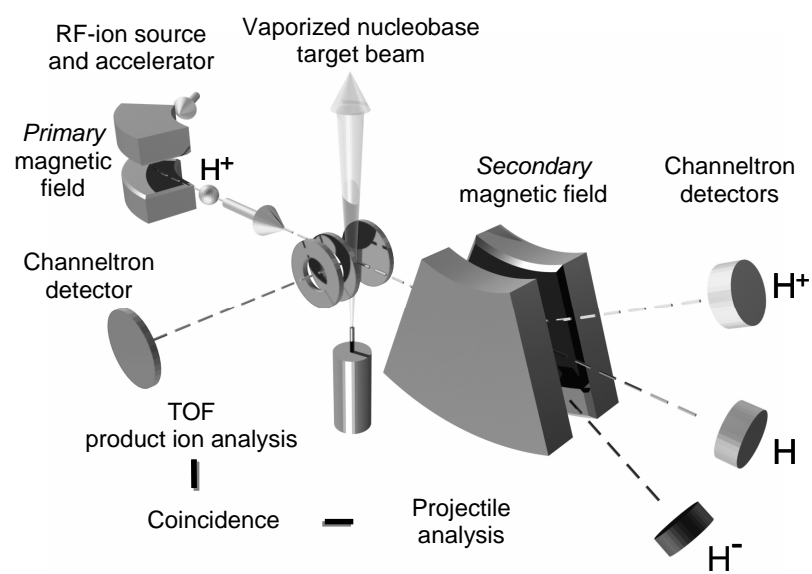
Fig. 5: Mass spectrum for proton impact ionization of thymine ($C_5H_6N_2O_2$, 126 amu) by electron capture and by direct ionization at 80 keV. The main ions expected to account for the peaks are listed in table 4.
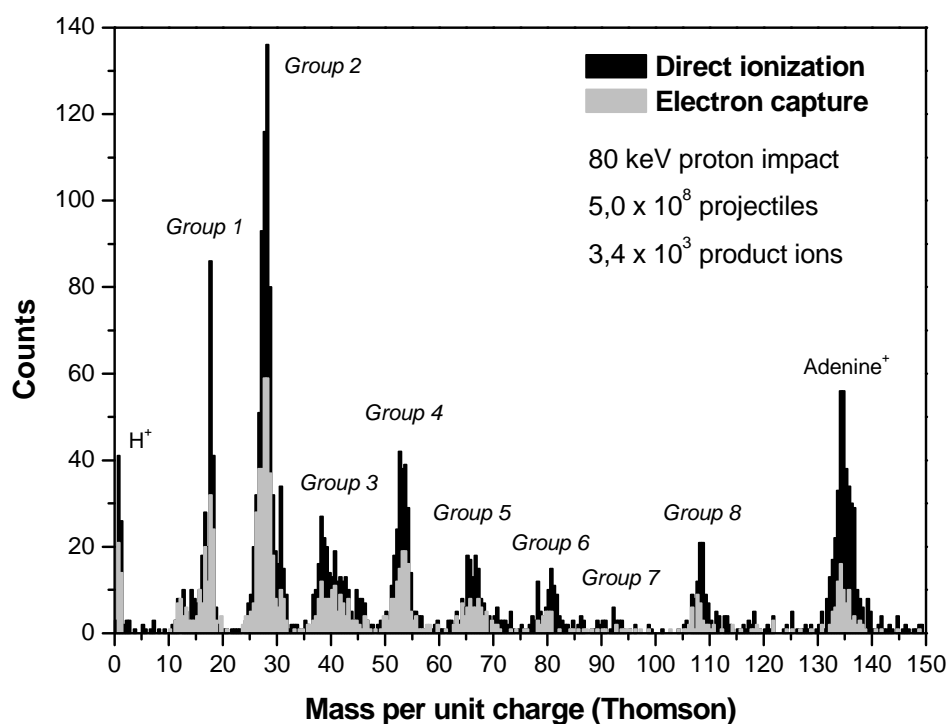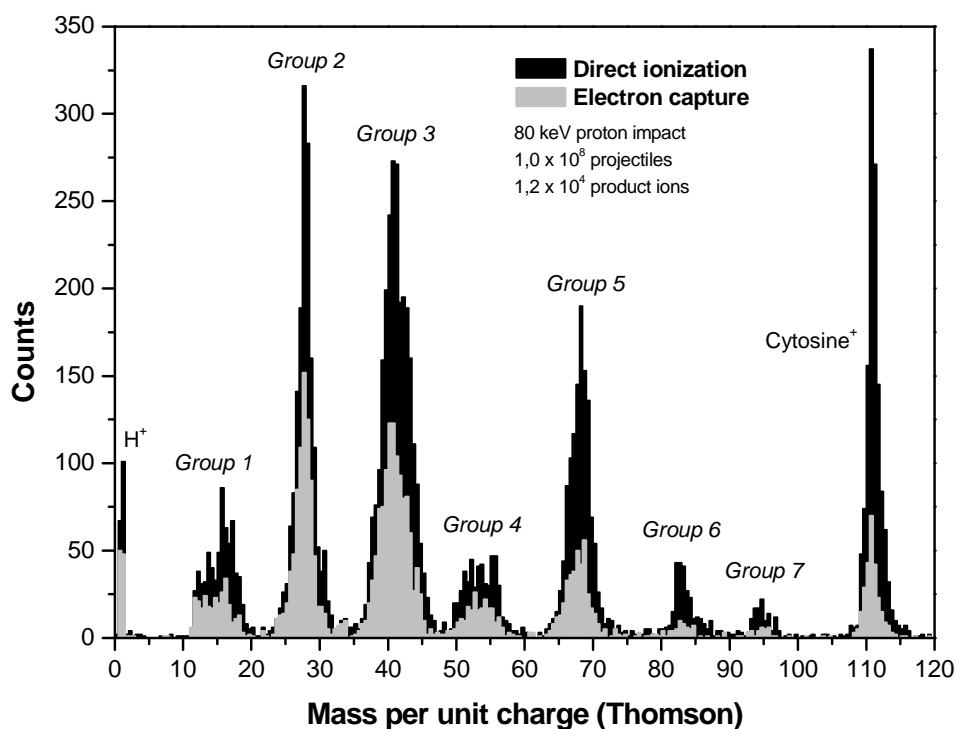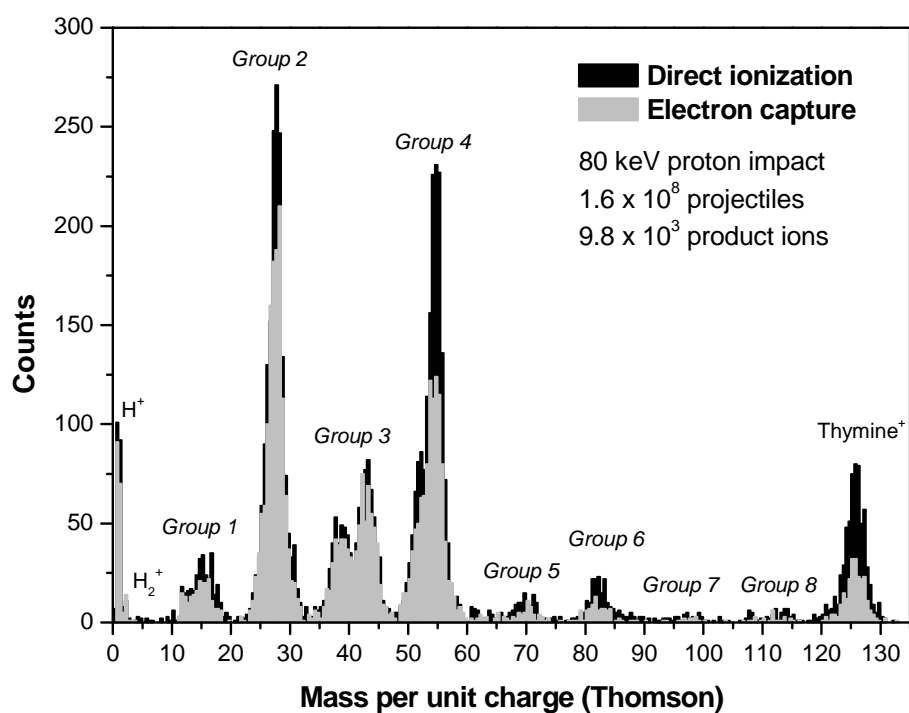
Table 1: Electron capture ionization branching ratios and ionization energies for adenine, thymine, and cytosine following proton impact at 80 keV ($1.8\ v_0$). The present results are compared with uracil [Tabet *et al.* unpublished] and water [Gobet *et al.* 2004, Shah *et al.* 2007].

Molecule	Electron capture / total ionization (%)	Ionization energy (eV)	Main fragment cation appearance energy (eV)
Adenine	27.1 ± 4 *(Present work)*	8.20 ± 0.03 [Jochims *et al.* 2005]	11.56 ± 0.05 ($C_4H_4N_4^+$, 108 Thomson) 12.8 ± 0.1 ($C_3H_3N_3^+$, 81) 13.1 ± 0.1 ($C_2H_4N_3^+$, 70) 13.2 ± 0.1 ($C_3H_2N_2^+$, 66) 13.7 ± 0.1 ($C_2H_2N_2^+$, 54) 13.0 ± 0.1 ($CH_3N_2^+$, 43) 14.0 ± 0.1 (CH_3N^+, 29) 13.1 ± 0.1 (CH_2N^+, 28) [Jochims *et al.* 2005]
Cytosine	27.6 ± 4 *(Present work)*	8.45 [Dougherty *et al.* 1978] [C]	*Unmeasured*
Thymine	26.6 ± 4 *(Present work)*	8.82 ± 0.03 [Jochims *et al.* 2005]	10.70 ± 0.05 ($C_4H_5NO^+$, 83) 13.20 ± 0.05 ($C_4H_4NO^+$, 82) 11.7 ± 0.1 ($C_3H_5N^+$, 55) 11.9 ± 0.1 ($CHNO^+$, 43) 14.4 ± 0.1 ($C_3H_3^+$, 39) 13.6 ± 0.1 (CH_2N^+, 28) [Jochims *et al.* 2005]
Uracil	25.4 ± 2 [Tabet *et al.* unpublished] [A]	9.15 ± 0.03 [Jochims *et al.* 2005]	10.95 ± 0.05 ($C_3H_3NO^+$, 69) 13.40 ± 0.05 ($C_3H_2NO^+$, 68) 13.6 ± 0.2 ($CHNO^+$, 43) 13.25 ± 0.05 ($C_2H_2O^+$, 42) 12.95 ± 0.05 (C_2HO^+ / $C_2H_3N^+$, 41) 14.06 ± 0.10 ($C_2H_2N^+$, 40) 13.75 ± 0.05 (CH_2N^+, 28) [Jochims *et al.* 2005]
Water	27.8 ± 2 [Gobet *et al.* 2004] [A, B] 25.7 [Shah *et al.* 2007] [C]	12.621 ± 0.002 [NIST]	18.08 ± 0.05 (OH^+) [Lafaivre and Marmet 1978] 19.0 (O^+) [Morrison and Traeger 1973] [C] 19.65 ± 0.05 (H^+) [Lafaivre and Marmet 1978]

[A] Measured with the same experimental system used to obtain the present results
[B] This result was corrected for differences in TOF transmission for the different product ions. As the relative production of fragment ions at this impact energy is greater for EC than for DI, correcting for acceptance tends to increase %EC results.
[C] No error estimation available

Table 2: Product ions observed following the ionization of gas-phase adenine by photon absorption [Jochims *et al.* 2005], electron impact [Rice *et al.* 1967], and proton impact (present work)

m/q in Thomson (with previous ion sum formula proposals)		
Ionization by 80 keV proton impact (present work) [A, B, C, D]	**Ionization by 70 eV electron impact** [Rice *et al.* 1967] [E]	**20 eV photo-ionization** (with proposed ion formula) [Jochims *et al.* 2005] [E]
134-136 (peak 135)		
	135	135 (adenine$^+$)
	134 – *weak*	134 ($C_5H_4N_5^+$)
	120 – *weak*	120 ($C_5H_4N_4^+$) - *weak*
		119 ($C_5H_3N_4^+$) - *weak*
107-109 (peak 109)		
	108	108 ($C_4H_4N_4^+$)
	107 – *weak*	107 ($C_4H_3N_4^+$)
		92 ($C_4H_2N_3^+$)
78-82 (peak 81)	81	81 ($C_3H_3N_3^+$)
	80	80 ($C_3H_2N_3^+$)
	70	70 ($C_2H_4N_3^+$)
64-68 (peak 66)	67	67 ($C_3H_3N_2^+$)
	66	66 ($C_3H_2N_2^+$)
	65	65 ($C_3HN_2^+$) - *weak*
52-54 (peak 53)	54	54 ($C_2H_2N_2^+$)
	53	53 ($C_2HN_2^+$)
37-42 (full range 36-47, peak 38)	43	43 ($CH_3N_2^+$)
	42 – *weak*	42 ($CH_2N_2^+$)
	41 – *weak*	41 (CHN_2^+)
	40	40 (CN_2^+) - *weak*
	39	39 (C_2HN^+) - *weak*
	38	38 (C_2N^+) - *weak*
30-31 (peak 31: $N_2H_3^+$)		
27-29 (peak 28)	29	29 (CH_3N^+)
	28	28 (CH_2N^+)
	27	27 (CHN^+)
18 (H_2O^+ impurity)		18 (H_2O^+) - *weak*
17 (OH^+ impurity)		17 (NH_3^+ / OH^+)- *weak*
Full range 12-16 (C^+, CH^+, N^+, NH^+, NH_2^+)	Not measured	14 (N^+) - *weak*
1 (H^+)		Not measured

[A] The same peak positions were observed for both direct ionization and electron capture.
[B] Unless stated otherwise, the ranges given above correspond to the half-maximum width of the DI peaks.
[C] The proton impact data only includes single ion production.
[D] Possible assignments for previously unobserved peaks.
[E] The channels labeled *weak* correspond to those reported by Jochims *et al.* [2005] and Rice et al. [1967] to have intensities < 5% of the maximum peak intensity.

Table 3: Product ions observed following the ionization of gas-phase cytosine by 80 keV (present work) and 100 keV [Le Padellec *et al.* 2008] proton impact and by 70 eV electron impact [Rice *et al.* 1965]

m/q in Thomson			Suggested ion sum formulae (principle peak assignments in bold)
70 eV electron impact [A] [Rice *et al.* 1966]	**100 keV proton impact** [C] [Le Padellec *et al.* 2008]	**80 keV proton impact** [B, D, E] (present work)	
111	111	110-111 (peak 111)	$C_4H_5N_3O^+$ (cytosine$^+$), $C_4H_4N_3O^+$
110 - *weak*			
95	95	93-96 (peak 95)	$C_4H_3N_2O^+$, $C_4H_5N_3^+$, $C_4H_2N_2O^+$, $C_4H_4N_3^+$
94 - *weak*			
84 - *weak*		82-84 (peak 83)	$C_2H_2N_3O^+$, $C_4H_5NO^+$, $C_2HN_3O^+$, $C_3H_5N_3^+$, $C_3H_4N_3^+$, $C_2N_3O^+$
83	83		
82 - *weak*			
70 - *weak*		66-70 (peak 68)	$C_2H_2N_2O^+$, $C_3H_3NO^+$, $C_3H_5N_2^+$, $C_3H_2NO^+$, $C_3H_4N_2^+$, $C_2N_2O^+$, $C_3H_3N_2^+$, $C_3H_2N_2^+$
69	69		
68	68		
67	67		
66	66*		
65 - *weak*			
57 - *weak*		50-57 (peaks at 53 and 55)	CN_2O^+, $C_2H_2NO^+$, $C_2H_3N_2^+$, $C_3H_4N^+$, $C_3H_3N^+$, $C_3H_2N^+$, C_3HN^+
56	56*		
55	55		
54 - *weak*			
53	53*		
52	52		
51	51*		
45 - *weak*			
44	44	39-43 (peak 41)	$CHNO^+$, CNO^+, $CH_2N_2^+$, $C_2H_4N^+$, CHN_2^+, $C_2H_3N^+$, $C_2H_2N^+$, CN_2^+, C_2HN^+
43	43		
42	42		
41	41		
40	40		
39	39		
38	38		
37 - *weak*			
32 - *weak*	32*		
	31*		
29	29	27-29 (peak 28)	CH_3N^+, CHO^+, CH_2N^+, CO^+, CHN^+, $C_2H_2^+$
28	28		
27	27*		
26	26*		
25 - *weak*	25*		
	18*	Full range 12-18 (peak 16)	H_2O^+ (impurity), OH^+, NH_2^+, O^+, NH^+, N^+, C^+,
	17		
	16*		
Not measured [F]	15		
	14		
	13		
	12		
	Not measured	1	H^+

[A] The channels labeled *weak* correspond to those reported by Rice *et al.* [1965] to have intensities < 5% of the maximum peak intensity.
[B] The same peak positions were observed for both direct ionization and electron capture.
[C] The non-asterisked product ion masses were labeled or mentioned explicitly by Le Padellec *et al.* [2004]. Conversely, the asterisked masses have been read from a published figure and are therefore subject to greater uncertainty.
[D] Unless stated otherwise, the ranges given above correspond to the half-maximum width of the DI peaks.
[E] The present proton impact data only includes single ion production.
[F] The 70 eV electron impact mass spectrum shown on the NIST database [NIST] includes ions in the range 12-18 Thomson.

Table 4: Product ions observed following gas-phase thymine ionization by photon absorption [Jochims *et al.* 2005], by 70 eV electron impact [Imhoff *et al.* 2005, Rice *et al.* 1965], and by 100 keV [Le Padellec *et al.* 2008] and 80 keV proton impact (present work).

m/q in Thomson (with previous ion sum formula proposals)				
Proton impact		70 eV electron impact		20 eV photo-ionization [Jochims *et al.* 2005] [F]
80 keV [A, B, C, D] (present work)	100 keV [E] [Le Padellec et al. 2008]	[Imhoff *et al.* 2005]	[Rice *et al.* 1967] [F]	
		128		
125-127 (peak 126)		127		
	126	126 Thymine+	126	126 Thymine+ ($C_5H_6N_2O_2^+$)
		125		125 ($C_5H_5N_2O_2^+$) - *weak*
		124		
108-114 (peak 112) $C_4H_4N_2O_2^+$, $C_4H_3N_2O_2^+$		112		
95-100 (peak 98)	97*	97	97 - *weak*	97 ($C_4H_3NO_2^+$) - *weak*
		84	84 - *weak*	84 ($C_4H_6NO^+$) - *weak*
80-84 (peak 82)	83*	83 ($C_4H_5NO^+$)	83	83 ($C_4H_5NO^+$)
	82	82 ($C_4H_4NO^+$)	82	82 ($C_4H_4NO^+$)
		81		
		80		
68-72 (peak 70)	71*	71	71 - weak	71 ($C_2HNO_2^+$) - *weak*
	70*	70	70 - weak	70 ($C_2H_2N_2O^+$) - *weak*
				58 (unassigned) - *weak*
53-56 (full range 49-59, peak 55)		56	56	56 ($C_3H_4O^+$)
	55	55 ($C_3H_5N^+$)	55	55 ($C_3H_5N^+$)
	54	54 ($C_3H_4N^+$)	54	54 ($C_3H_4N^+$)
		53	53	53 (unassigned) - *weak*
	52	52	52	52 (unassigned) - *weak*
		45		45 (unassigned) - *weak*
41-45 (peak 43)	44	44 (CH_2NO^+)	44	44 (CO_2^+ impurity)
	43	43	43 - *weak*	43 ($CHNO^+$) - *weak*
	42*	42		
		41	41 - weak	41 (unassigned) - *weak*
	40	40 ($C_3H_4^+$ / CN_2^+)	40	40 ($C_3H_4^+$)
37-40 (peak 39)	39	39 ($C_3H_3^+$)	39	39 ($C_3H_3^+$)
	38	38 ($C_3H_2^+$)	38 - *weak*	
		37 (C_3H^+)	37 - *weak*	
	29	29	29 - *weak*	29 (unassigned) - *weak*
26-29 (peak 28)	28 (CH_2N^+ / CO^+)	28 (CH_2N^+ / CO^+)	28	28 (CH_2N^+)
	27*	27 ($C_2H_3^+$ / CHN^+)	27	27 ($C_2H_3^+$ / CHN^+)
	26*	26 ($C_2H_2^+$)	26	26 ($C_2H_2^+$) - *weak*
	25*	25 (C_2H^+)		
18	18*	18 (H_2O^+)		
	17 (OH^+)	17 (OH^+)		
	16*	16 (CH_4^+ / O^+)		
12-17 (peak 15)	15 (NH^+)	15 (CH_3^+)	Not measured	Not measured
	14 (N^+)	14 (CH_2^+)		
	13 (CH^+)	13 (CH^+)		
	12 (C^+)	12 (C^+)		
2	Not measured	2 (H_2^+)		
1		1 (H^+)		

[A] The same peak positions were observed for both direct ionization and electron capture.
[B] Unless stated otherwise, the given ranges correspond to the half-maximum width of the DI peaks.
[C] The proton impact data only includes single ion production.
[D] Ion formula proposals are given for previously unobserved or unassigned peaks.
[E] The non-asterisked product ion masses were labeled or mentioned explicitly by Le Padellec *et al.* [2004]. Conversely, the asterisked masses have been read from a published figure and are therefore subject to greater uncertainty (the feature centered 97 Thomson is particularly weak and uncertain).
[F] The channels labeled *weak* correspond to those reported by Jochims *et al.* [2005] and Rice *et al.* [1965] to have intensities < 5% of the maximum peak intensity.

Table 5: Product ion fragmentation ratios (the number of ions detected in a given m/q range over the total number of ions detected) for 80 keV proton collisions with gas-phase adenine, thymine, cytosine, and uracil [Tabet *et al.* unpublished]. Background noise has been removed and the ions produced by electron capture (EC) and by direct ionization (DI) have been given separately.

Molecule	% (fragment ion production / total ionization)																						
	H⁺		H₂⁺		Group 1 10≤ m/q <20 ᴬ		Group 2 20≤ m/q <35		Group 3 35≤ m/q <47		Group 4 47≤ m/q <60		Group 5 60≤ m/q <75		Group 6 75≤ m/q <90		Group 7 90≤ m/q <105		Group 8 105≤ m/q <115		M⁺ group	
	EC	DI	EC	DI	EC	DI	EC	DI	EC	DI	EC	DI	EC	DI	EC	DI	EC	DI	EC	DI	EC	DI
Adenine (M = 135)	3.3 ± 0.6	2.7 ± 0.7	0.0 ± 0.1	0.1 ± 0.2	14.6 ± 1.3	10.9 ± 1.4	32.1 ± 2.1	28.9 ± 2.5	12.2 ± 1.2	10.8 ± 1.3	12.5 ± 1.2	10.7 ± 1.2	7.5 ± 0.9	6.8 ± 1.0	3.2 ± 0.6	4.7 ± 0.8	1.2 ± 0.4	1.0 ± 0.5	3.8 ± 0.6	4.8 ± 0.7	**8.4 ± 1.0**	**17.2 ± 1.6**
Thymine (M = 126)	4.1 ± 0.3	3.4 ± 0.6	0.5 ± 0.1	0.3 ± 0.2	4.9 ± 0.4	5.1 ± 0.7	32.8 ± 1.0	28.5 ± 1.7	19.9 ± 0.8	15.7 ± 1.0	26.7 ± 0.9	29.0 ± 1.6	2.0 ± 0.2	2.5 ± 0.5	2.2 ± 0.2	3.4 ± 0.5	0.4 ± 0.1	0.7 ± 0.3	0.6 ± 0.1	1.1 ± 0.3	**5.9 ± 0.4**	**10.7 ± 0.8**
Cytosine (M = 111)	2.9 ± 0.3	1.9 ± 0.2	0.0 ± 0.1	0.0 ± 0.1	8.5 ± 0.5	7.6 ± 0.6	25.1 ± 1.0	19.5 ± 0.8	33.9 ± 1.2	29.7 ± 0.9	6.9 ± 0.5	6.4 ± 0.4	11.5 ± 0.6	14.7 ± 0.6	2.1 ± 0.3	3.5 ± 0.3	1.0 ± 0.2	1.5 ± 0.2	-		**8.1 ± 0.5**	**15.1 ± 0.6**
Uracil ᴮ (M = 112)	2.7 ± 0.3	1.5 ± 0.3	0.0 ± 0.1	0.0 ± 0.1	6.9 ± 0.6	5.0 ± 0.5	24.9 ± 1.1	22.3 ± 1.0	40.2 ± 1.5	37.5 ± 1.0	3.6 ± 0.4	2.9 ± 0.3	11.2 ± 0.7	14.2 ± 0.7	0.6 ± 0.2	0.7 ± 0.2	0.2 ± 0.1	0.2 ± 0.2	-		**9.6 ± 0.7**	**15.5 ± 0.7**

The errors given in the table are purely statistical; the transmission of the TOF mass spectrometer has not been taken into account.
Group m/q ranges are given in Thomson
M = nucleobase mass in amu
For all the nucleobases, no evidence was observed for fragment ion production above the background noise for masses in the range 2.5 < m/q < 10 Thomson
For adenine, no evidence was observed for fragment ion production above the background noise for masses in the range 115 < m/q < 125 Thomson
ᴬ This group may contain contributions due to water impurities in the jet. In particular, this is expected to account for the high ion yields in this range for adenine.
ᴮ Tabet *et al.* [unpublished]